

Article

# Interaction between Ni/Ti Nanomultilayers and Bulk Ti-6Al-4V during Heat Treatment

André João Cavaleiro <sup>1,2,\*</sup>, Ana Sofia Ramos <sup>1</sup>, Francisco Braz Fernandes <sup>3</sup>, Carsten Baehtz <sup>4</sup> and Maria Teresa Vieira <sup>1</sup>

<sup>1</sup> CEMMPRE, Department of Mechanical Engineering, University of Coimbra, R. Luís Reis Santos, 3030-788 Coimbra, Portugal; sofia.ramos@dem.uc.pt (A.S.R.); teresa.vieira@dem.uc.pt (M.T.V.)

<sup>2</sup> INEGI, Instituto de Ciência e Inovação em Engenharia Mecânica e Engenharia Industrial-INEGI, Campus da FEUP, 400 4200-465 Porto, Portugal

<sup>3</sup> CENIMAT/I3N, Department of Materials Science, Faculty of Sciences and Technology, Universidade Nova de Lisboa, Campus de Caparica, 2829-516 Caparica, Portugal; fbf@fct.unl.pt

<sup>4</sup> Helmholtz Zentrum Dresden Rossendorf HZDR, Institute of Ion Beam Physics and Materials Research, D-01314 Dresden, Germany; baehtz@esrf.fr

\* Correspondence: andre.cavaleiro@dem.uc.pt; Tel.: +351-239790700

Received: 2 October 2018; Accepted: 25 October 2018; Published: 27 October 2018



**Abstract:** The diffusion bonding of Ti-6Al-4V to NiTi alloys assisted by Ni/Ti reactive multilayer thin films indicates the diffusion of Ni from the filler material towards bulk Ti-6Al-4V. As a consequence, the fragile NiTi<sub>2</sub> intermetallic phase is formed at the joint interface. In this context, the aim of this work is to investigate the occurrence of Ni diffusion from Ni/Ti nanomultilayers towards Ti-6Al-4V substrates. For this purpose, multilayer coated Ti alloys were studied in situ at increasing temperatures using synchrotron radiation. After heat treatment, scanning electron microscopy (SEM) analyses were carried out and elemental map distributions were acquired by electron probe microanalysis (EPMA). The EPMA maps confirm the occurrence of Ni diffusion; the presence of Ni in the substrate regions immediately underneath the nanomultilayers is clearly indicated and becomes more pronounced as the temperature increases. The presence of Ni is observed in the same locations where V is found, thus in  $\beta$ -Ti grains of Ti-6Al-4V. At the same time, the synchrotron results together with SEM analyses allow the increase of the amount of  $\beta$ -Ti phase in Ti-6Al-4V to be identified, while the thin films are mainly constituted by NiTi<sub>2</sub>. Therefore, the presence of the brittle NiTi<sub>2</sub> intermetallic phase can be avoided if Ni diffusion is prevented.

**Keywords:** Ni/Ti; multilayers; Ni; Ti-6Al-4V; diffusion

## 1. Introduction

Due to their high strength to weight ratio and good corrosion resistance, titanium and titanium based alloys have a wide range of applications, such as in aerospace and biomedical industries. The Ti-6Al-4V alloy, constituted by  $\alpha$ -Ti grains surrounded by  $\beta$ -Ti grains, accounts for about 60% of the total titanium production because it is easy to work with and it presents good mechanical properties due to the  $\alpha/\beta$  alloy duality [1]. In order to have  $\beta$ -Ti at room temperature it is necessary to add beta stabilizing elements, such as vanadium. There are two different groups of  $\beta$  alloying elements:  $\beta$ -isomorphous and  $\beta$ -eutectoid. Vanadium, which is  $\beta$ -isomorphous, has high solubility in titanium and as the V content increases the  $\beta$  phase will also increase. On the contrary, since nickel is a  $\beta$ -eutectoid element, beside  $\beta$ -Ti it leads to the formation of intermetallic compounds, even for low Ni contents [2].

To enlarge its field of application, appropriate techniques for joining Ti-6Al-4V to itself and to other materials, in particular to NiTi shape memory alloys, must be developed. However, joining of Ti

alloys is difficult due to their high reactivity. The formation of oxides and brittle intermetallics can reduce joint strength. In particular, dissimilar joining can be challenging and often a filler material is required. Several joining attempts have been made by laser welding [3–5], brazing [6,7] and diffusion bonding [8–10]. Regarding the dissimilar diffusion bonding of Ti-6Al-4V, it is common to introduce metal foils as intermediate material [11]. In this context, to enhance the Ti-6Al-4V and NiTi diffusion bonding process, Ni/Ti multilayer thin films have been used [12,13]. These previous works reveal the formation of NiTi<sub>2</sub> at the bonding interface during the joining process. The presence of the brittle NiTi<sub>2</sub> phase led to joint failure. In order to increase joint strength, it is necessary to understand the mechanism behind the formation of the NiTi<sub>2</sub> phase and the role of the Ti-6Al-4V alloy. The NiTi<sub>2</sub> phase was detected by in situ synchrotron X-ray diffraction of Ni/Ti multilayers deposited onto Ti6Al4V [14]. After heat treatment (HT), the NiTi<sub>2</sub> phase was observed close to the Ti-6Al-4V substrate by transmission electron microscopy [14]. However, using conventional high-temperature X-ray diffraction, the formation of NiTi<sub>2</sub> in Ni/Ti multilayer thin films deposited onto stainless steel was not identified [15]. In a recent paper, Chen et al. [16] studied the diffusion behavior in Ti-6Al-4V alloys modified by the deposition of Cu/Ni bilayers using the electroplate method. The diffusion of Cu/Ni/Ti was significantly influenced by the HT temperature and caused the formation of several intermetallic phases, including NiTi, NiTi<sub>2</sub>, and Ni<sub>4</sub>Ti<sub>3</sub> at the Ni/Ti interface. In addition, the Ni layer could not prevent diffusion of Ti towards the Cu side [16].

The aim of this study is to understand the interaction between Ni and Ti-6Al-4V during heat treatment, to clarify the mechanism behind the formation of the NiTi<sub>2</sub> phase during diffusion bonding using Ni/Ti multilayer thin films. Two different Ni/Ti nanomultilayer configurations were deposited onto bulk Ti-6Al-4V. The bulk and filler materials were analyzed in situ using synchrotron X-ray diffraction during heat treatment at temperatures typical of those used in diffusion bonding. The evolution of the Ni/Ti nanomultilayers and the interaction with the Ti-6Al-4V substrate as a function of temperature were evaluated using scanning electron microscopy and elemental map distributions.

## 2. Experimental Details

### 2.1. Deposition Technique

Ti-6Al-4V from Goodfellow with a 2 mm thickness was cut into uniform 10 × 10 mm substrates. The substrates were polished up to 1 μm diamond suspension.

Ni/Ti reactive multilayer thin films with a total thickness close to 2.5 μm were deposited onto the polished Ti-6Al-4V substrates using a dual cathode magnetron sputtering equipment (Hartec, Stetten am kalten Markt, Germany). The substrates were mounted on a rotating copper block which acts as a heat sink, to avoid diffusion during the deposition process. The time that the substrates under rotation pass in front of each target, and consequently the individual layer thicknesses, depends on the substrates' rotation speed. The deposition chamber was evacuated to approximately  $3 \times 10^{-4}$  Pa. Ni and Ti nanolayers were deposited by magnetron sputtering at 0.35 Pa from pure Ti (99.99%) and Ni (99.98%) targets. In order to obtain near equiatomic overall chemical compositions, the target power density used for the Ti and for Ni were  $5.1 \times 10^{-2}$  W·mm<sup>-2</sup> and  $2.5 \times 10^{-2}$  W·mm<sup>-2</sup>, respectively. The magnetic Ni target had a reduced thickness of 1 mm. Multilayer thin films with 12 and 25 nm periods (bilayer thicknesses) were deposited by using different substrate rotation speeds.

In order to understand the NiTi<sub>2</sub> phase formation, two different configurations were studied: Ni/Ti multilayer thin films with periods of 12 and 25 nm were deposited onto Ti-6Al-4V with or without a tungsten interlayer. Ni was always the first layer of the Ni/Ti films. The W interlayer was ~12 nm thick. The diffusivity of Ni in tungsten is extremely reduced, suggesting that it can be used as a Ni diffusion barrier. In addition, W is also almost insoluble in the NiTi phase [17]. It should be noted that NiTi is the first phase to form upon heat treatment of Ni/Ti multilayers with nanometric

periods [14,18]. Due to its atomic characteristics, tungsten is excellent for contrast, particularly in backscattered electron (BSE) scanning electron microscopy (SEM).

## 2.2. Characterization Technique

The phase evolution of the system with temperature was studied by synchrotron X-ray diffraction (XRD), in scanning mode, at the Materials Research station of the Rossendorf beam line in the European Synchrotron Radiation Facility (ESRF, Grenoble, France). The coated Ti-6Al-4V substrates were placed in a furnace mounted on a six-circle goniometer. The incident X-ray beam was monochromatized to 11.5 keV ( $\lambda = 0.1078$  nm). A micro-strip detector system (Mythen) for time-resolved experiments with high angular accuracy was used. Steps of 50 °C were implemented up to the desired maximum temperature (850 or 900 °C). At each temperature step,  $\theta$ -2 $\theta$  isothermal scans ( $20^\circ < 2\theta < 42^\circ$ ) were acquired.

After the heat treatment carried out during the in situ XRD analysis, elemental distribution maps were obtained by electron probe microanalysis (EPMA) using a five-spectrometer Cameca SX 50 (CAMECA, Gennevilliers, France) equipment in order to visualize the relative variation of element concentrations as a result of diffusion. Scanning electron microscopy was used to characterize the heat treated coated Ti-6Al-4V. For comparison purposes, SEM after low temperature HT (600 °C) was also carried out. The analyses were performed at a 15 kV acceleration voltage in secondary and backscattered electron modes using a field emission gun FEI QUANTA 400F (FEI Company, Hillsboro, OR, USA) high-resolution SEM. The cross-sections for EPMA and SEM analyses were prepared by cutting the heat treated samples and mounting them transversely in resin. Following this, standard metallographic preparation was conducted to obtain flat and smooth surfaces.

## 3. Results

### 3.1. In Situ Characterization during Heat Treatment

The Ni/Ti films were analyzed using the synchrotron based high-temperature X-ray diffraction procedure described. Figures 1 and 2 present the phase evolution with temperature of the Ni/Ti films under study. It is important to notice that at the bottom of the XRD figures the diffraction peaks indicated for the different phases were based on ICDD (International Centre for Diffraction Data) standards collected at room temperature. Therefore, some deviation to low diffraction angles is expected as the temperature increases. The  $\beta$ -Ti peak presents a deviation to high diffraction angles due to residual stresses, since the  $\beta$ -Ti phase growth is trapped between  $\alpha$ -Ti grains. For the multilayers with a Ni bottom layer (Figure 1), the evolution towards the B2-NiTi phase is similar to the multilayers starting with Ti, previously studied up to 600 °C [14]. However, in the present case, as the temperature increases the intensity of the B2-NiTi main diffraction peak diminishes and the NiTi<sub>2</sub> peak increases, suggesting a possible compromise between the formation of one phase and the decrease of the other. Moreover, the  $\beta$ -Ti peak shows a significant increase for high HT temperatures. These results can be explained by the diffusion of Ni from the thin film towards the Ti-6Al-4V alloy. For the 12 nm period multilayer (Figure 1a), no B2-NiTi peak can be discerned at the highest temperature (real temperature = 712 °C); only substrate and NiTi<sub>2</sub> peaks can be identified, indicating that at this temperature the phase evolution is complete. At temperatures above 700 °C, besides the diffusion of Ni, the diffusion of Ti from Ti-6Al-4V towards the thin films becomes important, especially for the lowest period multilayer which has an increased diffusivity. Therefore, at 712 °C for the 12 nm period multilayer, the thin film is only constituted by the NiTi<sub>2</sub> Ti-rich phase. Although the 25 nm period multilayer reached higher temperatures (real temperature = 772 °C) than the 12 nm period multilayer, the larger grain size, and consequently lower reactivity, may explain why it was still possible to identify residual B2-NiTi at the maximum temperature. As the temperature reaches  $\approx 750$  °C, the  $\beta$ -Ti peak becomes significant.

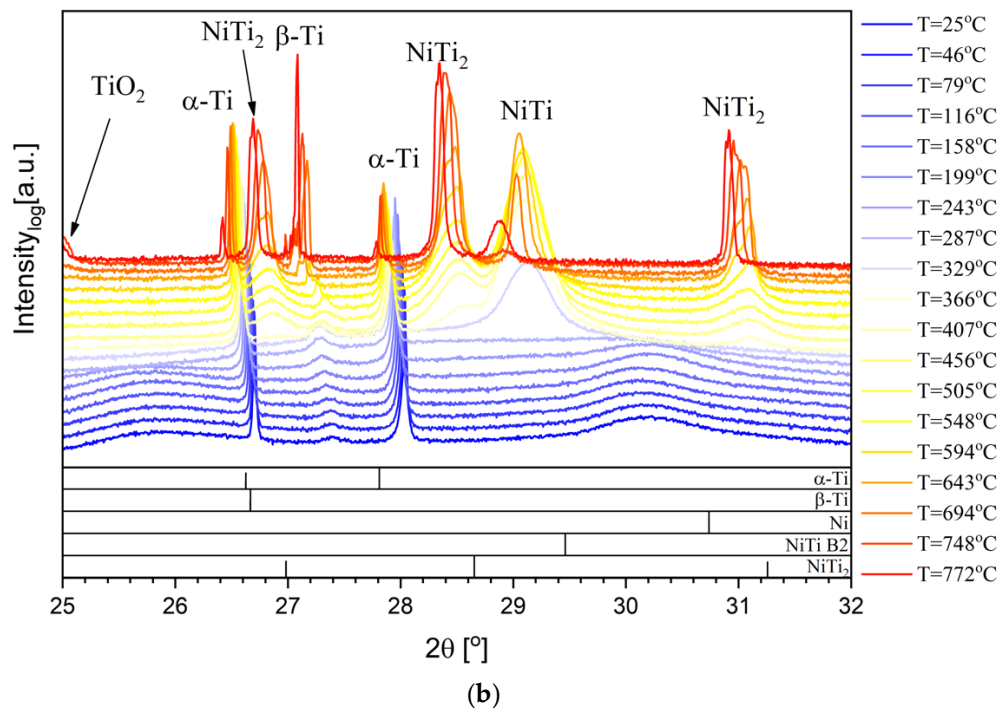
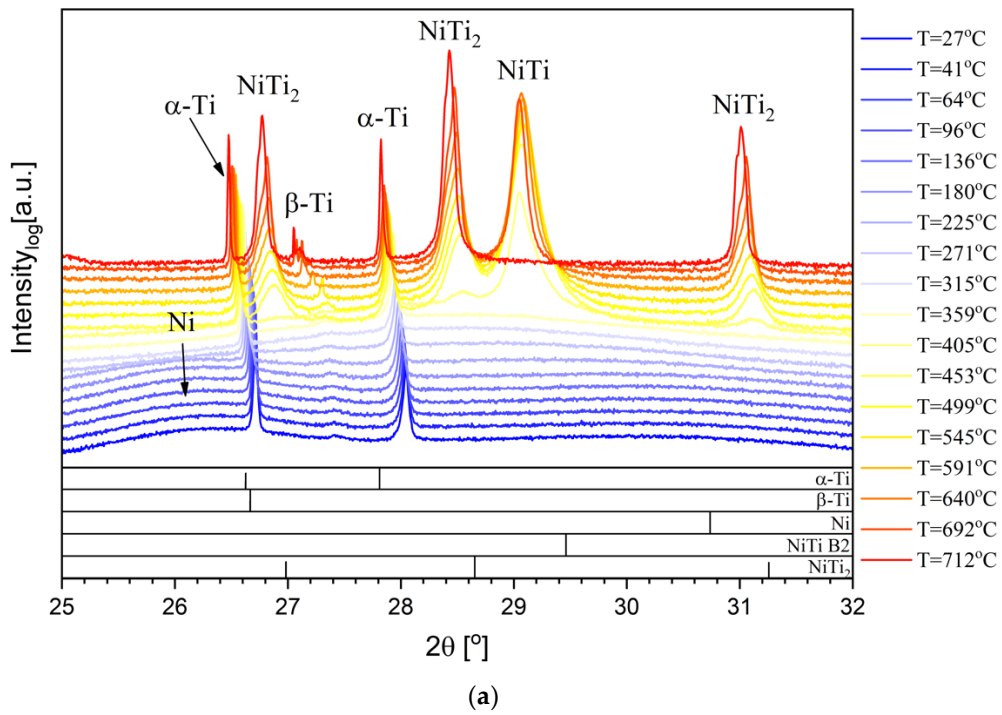


**Figure 1.** In situ synchrotron XRD phase evolution of multilayer thin films with (a) 12 nm and (b) 25 nm period.

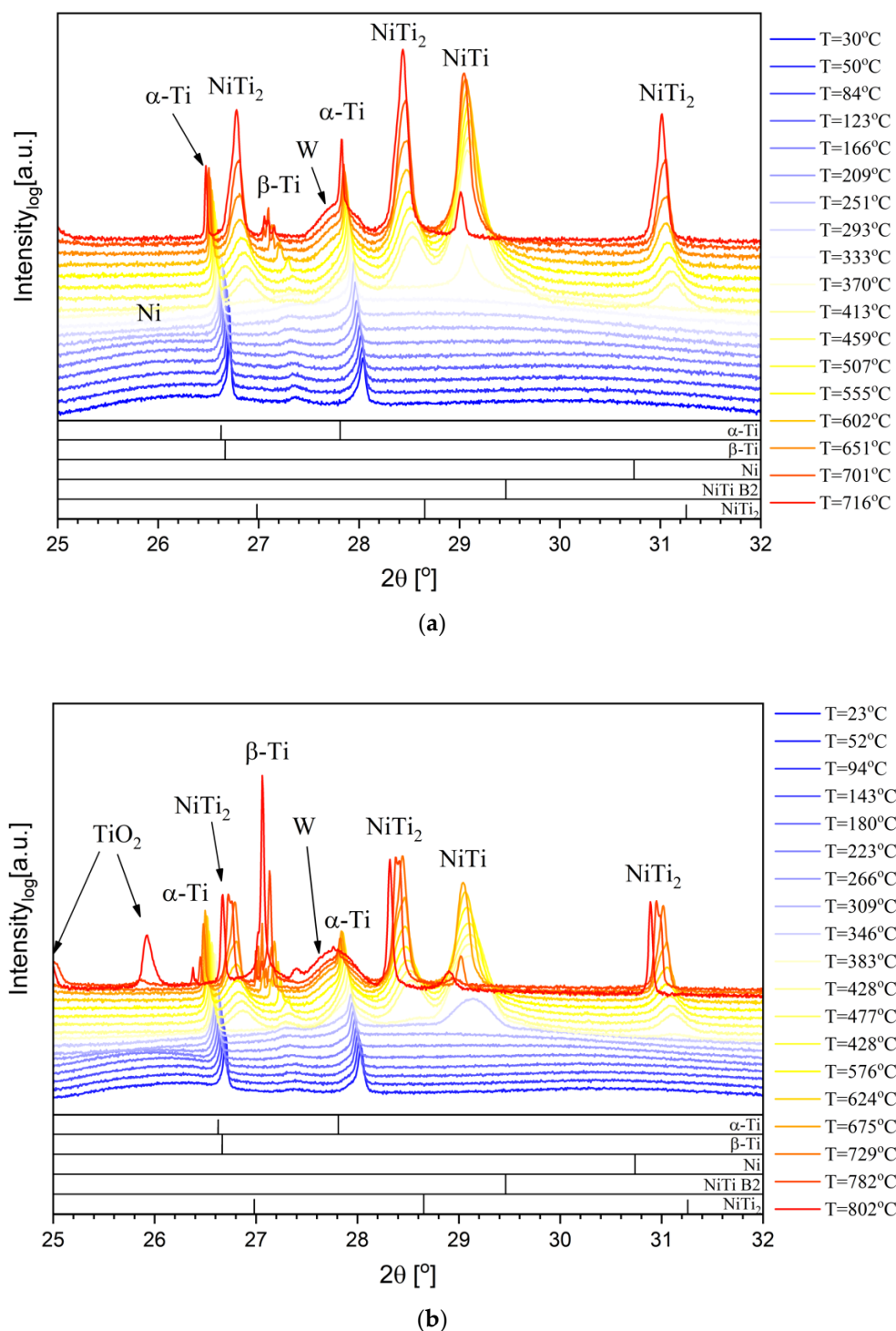


**Figure 2.** In situ synchrotron XRD phase evolution of multilayer thin films (W interlayer) with (a) 12 nm and (b) 25 nm period.

With or without W interlayer the structural evolution with temperature is similar (Figure 2). However, for films with  $\Lambda = 12$  nm the B2-NiTi phase was still distinguishable at the maximum HT temperature (real temperature = 716 °C), meaning that the tungsten might have changed the Ni diffusion kinetics.

The photon absorption coefficient for 11.5 keV is  $\approx 1.1 \times 10^4 \text{ mm}^2 \cdot \text{g}^{-1}$  and  $\approx 2.1 \times 10^4 \text{ mm}^2 \cdot \text{g}^{-1}$  for Ti and Ni, respectively [19]. Since for compounds and mixtures the absorption is averaged using the weight content of each component, if the weight ratio increases in a lower absorption element (in

this case, Ti), the overall absorption decreases. Before the phase transformation, the Ni/Ti multilayer thin films are near equiatomic, and at the end of the thermal cycle the NiTi<sub>2</sub> is the dominant phase, resulting in less absorption and enabling photons to reach the tungsten layer. The differences in photon absorption explain why at the beginning of the heat treatment the presence of W is not detected and, as soon as the NiTi<sub>2</sub> is formed, the tungsten peak starts to emerge.

Based on the synchrotron results, with or without W interlayer, it can be concluded that the formation of NiTi<sub>2</sub> is related with the disappearance of the B2-NiTi phase as well as with the formation of  $\beta$ -Ti. A possible explanation can be related with the diffusion of Ni from the multilayer thin film towards the bulk Ti-6Al-4V, because Ni is a  $\beta$ -titanium element. Since this element is a titanium  $\beta$ -eutectoid, it signifies that besides increasing the  $\beta$ -Ti phase, Ni should also promote the formation of NiTi<sub>2</sub> on Ti-6Al-4V.

In this study, the Ni<sub>4</sub>Ti<sub>3</sub> phase was not detected, as in the study of Chen et al. [16], due to the different coating chemical composition, configuration (nanoscale multilayer versus microscale bilayer), and processing technology.

### 3.2. Ex Situ Characterization after Heat Treatment

Figure 3 shows the presence of  $\beta$ -phase in the grain boundaries of  $\alpha$ -Ti (dark-phase); neither the period nor the presence of the W interlayer seems to influence this microstructure after HT at 600 °C. However, the amount of  $\beta$ -phase increases after HT at temperatures higher than 600 °C (Figures 3 and 4).  $\beta$ -Ti is much more evident close to the interface thin film/bulk material, which is attributed to the diffusion of Ni from the film towards Ti-6Al-4V. As a consequence, the films become depleted in Ni, giving rise to the formation of NiTi<sub>2</sub> as already confirmed by synchrotron XRD. The SEM (BSE) images clearly reveal the presence of the W interlayer (bright lines in Figures 4b and 5b), which remains intact, even after HT, indicating unequivocally the initial location of the interface film/substrate. In the presence of the W interlayer, the 12 nm period multilayer image shows that when the NiTi<sub>2</sub> rich film is in direct contact with a  $\beta$ -Ti grain, the connection will be the preferential route for the Ni diffusion, while if the NiTi<sub>2</sub> only contacts the  $\alpha$ -Ti phase, the NiTi<sub>2</sub> will grow over the W interlayer (Figure 4b). As expected, Ni preferentially diffuses towards the  $\beta$ -phase. Ni is a  $\beta$ -titanium element and due to the different crystallographic structures ( $\beta$ -Ti is bcc while  $\alpha$ -Ti is hcp), Ni diffusion is considerably higher on the  $\beta$ -Ti phase than in  $\alpha$ -Ti. Regarding the film with a 25 nm period, the cross-section is similar without and with W interlayer (Figure 5). It should be noted that the 25 nm period films were treated at higher temperatures (900 °C), and it is probable that the W could not prevent the Ni diffusion. The increase of the HT temperature leads to deeper Ni diffusion, with film and substrate becoming almost indiscernible. Simultaneously, the presence of  $\alpha$ -Ti significantly decreases (dark regions).

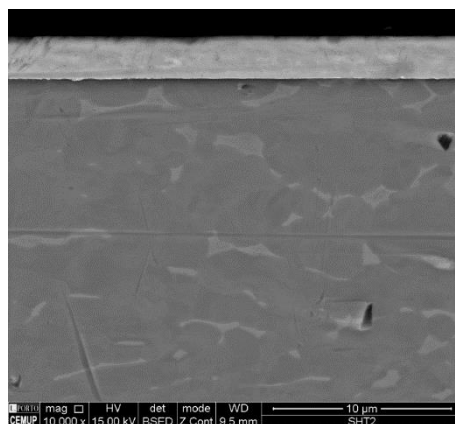


**Figure 3.** Cross-section SEM backscattered electron (BSE) image of a Ni/Ti multilayer thin film (W interlayer) with 12 nm period after heat treatment (HT) at 600 °C.

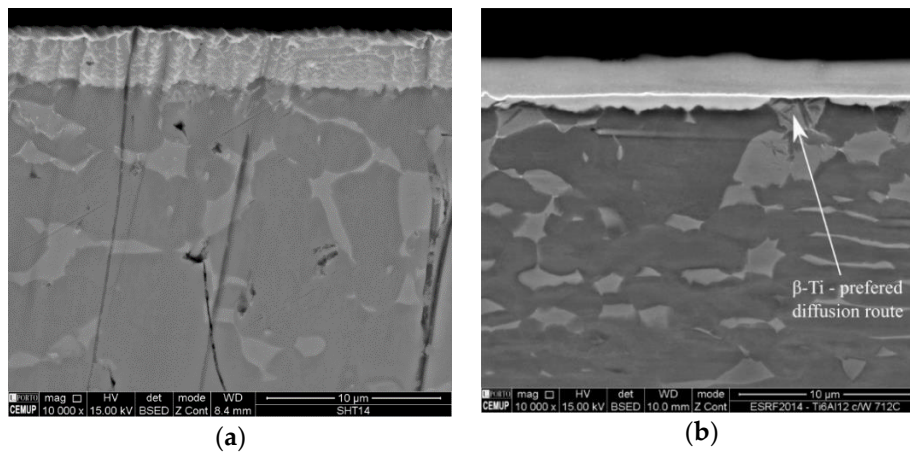


**Figure 4.** Cross-section SEM BSE images of Ni/Ti multilayer thin films with 12 nm period (a) without or (b) with W interlayer after HT at 850 °C.

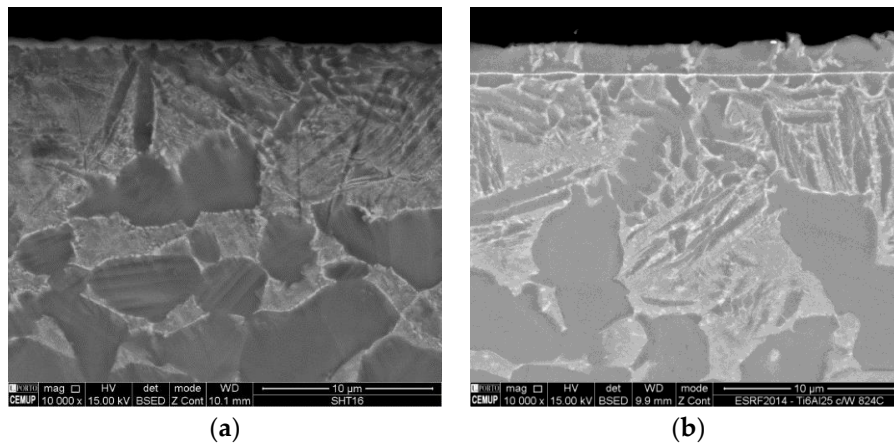


**Figure 5.** Cross-section SEM BSE images of Ni/Ti multilayer thin films with 25 nm period (a) without or (b) with W interlayer after HT at 900 °C.

In order to analyze the diffusion phenomena in detail, cross-sections of the heat treated films were prepared and elemental (V, Ni and W) distributions over areas with  $50 \times 50 \mu\text{m}^2$  were carried out by EPMA (Figures 6 and 7). The cross-sections were analyzed starting from the thin film/substrate interface to the Ti-6Al-4V bulk material, to avoid the steep Ni increase due to the film. In Figures 6 and 7, for each map the color scale is independent (from low concentration purple to high concentration red). As previously mentioned, in Ti-6Al-4V vanadium is added to induce the formation of the  $\beta$ -Ti phase, therefore this element can be used as a trace element for the location of this phase. From the elemental map distribution, it is possible to identify the vanadium in the  $\beta$ -Ti and this phase is distributed around  $\alpha$ -Ti grains. The tungsten distribution maps do not show any diffusion of W towards the Ti-6Al-4V substrate.

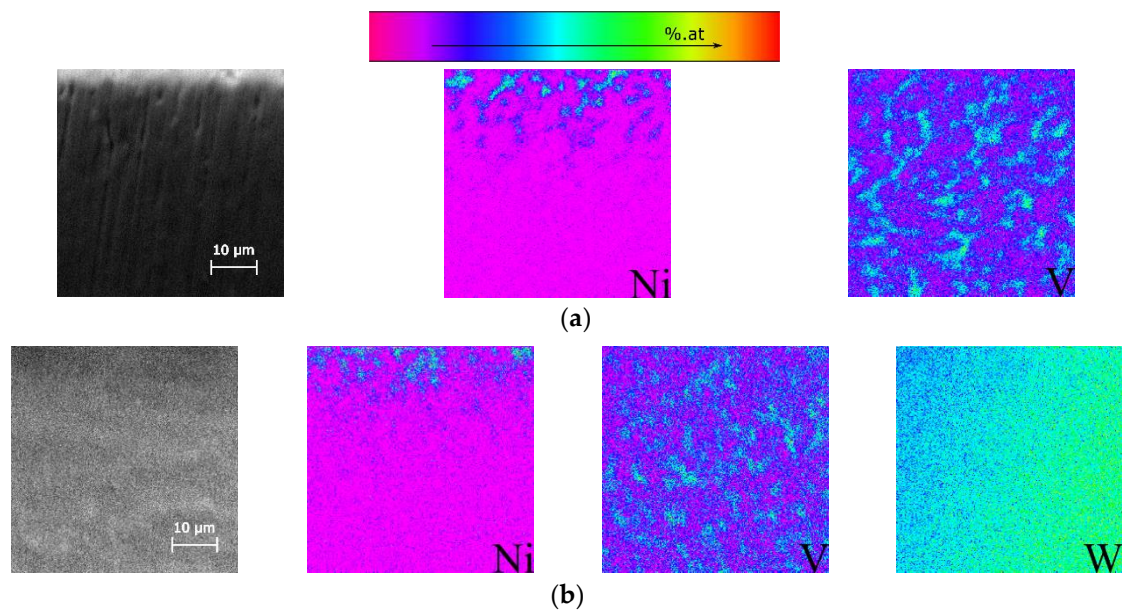


**Figure 6.** Electron probe microanalysis (EPMA) elemental map distributions of the zone directly under the heat treated Ni/Ti multilayer thin films with 12 nm period (a) without or (b) with W interlayer.

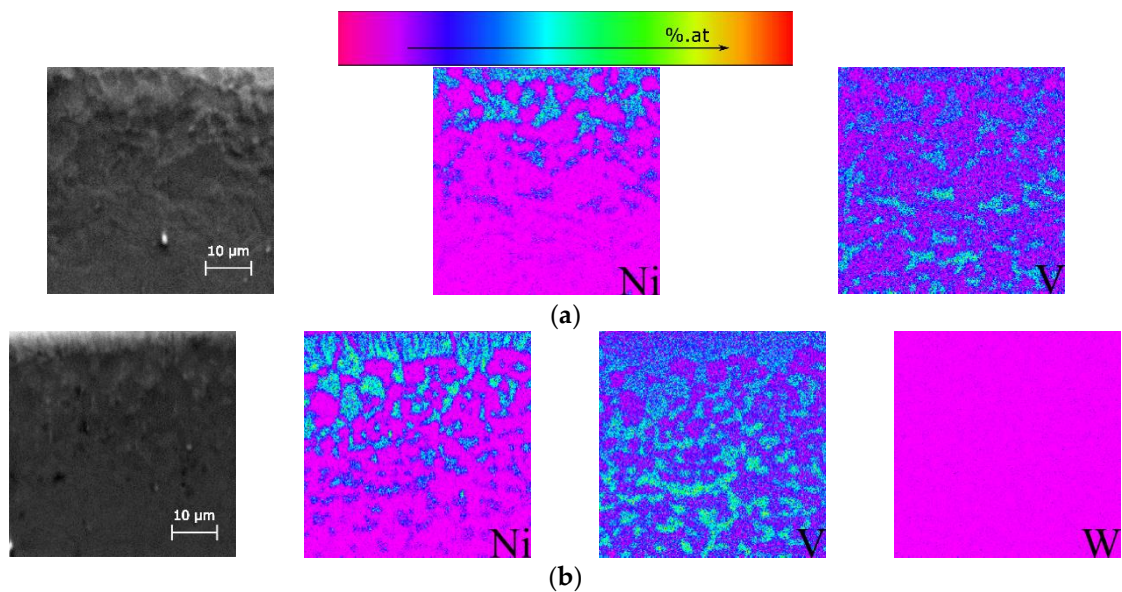


**Figure 7.** EPMA elemental map distributions of the zone directly under the heat treated Ni/Ti multilayer thin films with 25 nm period (a) without or (b) with W interlayer.

The nickel distribution maps show that this element clearly diffuses to the same locations where V is detected (the  $\beta$ -Ti grains). Independent of the multilayer configuration, as the temperature increases, the Ni diffusion length increases. For the 12 nm period multilayer the maximum temperature was the same without and with interlayer, and even though the Ni diffusion length is almost the same, with the W interlayer the Ni diffusion length is slightly shorter (Figure 6). The small difference in the diffusion lengths confirms that the W interlayer works as a barrier, but since its thickness is relatively small ( $\approx 12$  nm) it is not effective enough to completely prevent Ni migration. In the similar analysis of Ni/Ti multilayer thin films, starting with titanium and heat treated at lower temperatures ( $\leq 500$  °C), it was not possible to identify any Ni diffusion, indicating that a minimum temperature must be reached in order to promote the diffusion of Ni towards the  $\beta$ -Ti phase ( $\sim 700$  °C for 12 nm period and  $\sim 750$  °C for 25 nm). For the 25 nm period multilayer, the temperatures reached were higher, and as a

consequence Ni diffusion is more pronounced and the amount of  $\beta$ -Ti phase also increases (Figure 7). For this period, the effect of the W interlayer cannot be evaluated because the temperature reached was different without and with interlayer. With the W interlayer, the sample attained 802 °C and the region adjacent to the thin film is only composed of  $\beta$ -Ti, as indicated by the V map. Once again it is confirmed that Ni diffuses to  $\beta$  grains and that the diffusion depth increases with temperature. According to Figure 7b, it is possible to find Ni up to a depth of close to 50  $\mu$ m. The fact that Ni diffusion can be clearly observed as the temperature increases, and that  $\beta$ -Ti and NiTi<sub>2</sub> phases can be clearly identified by XRD and SEM concurrently, confirms that the NiTi<sub>2</sub> phase formation is directly related to the Ni diffusion process. Therefore, if an effective barrier is placed between Ni/Ti nanomultilayers and Ti-6Al-4V substrates, it would be possible to prevent Ni diffusion and avoid the formation of the brittle NiTi<sub>2</sub> intermetallic compound. This would be particularly important when using Ni/Ti multilayer thin films to assist the similar and dissimilar diffusion bonding process of  $\alpha/\beta$  Ti alloys.

#### 4. Conclusions

During heat treatment of Ti-6Al-4V coated with Ni/Ti nanomultilayers, Ni diffusion from the thin films towards the bulk material is promoted. According to the results, the occurrence of Ni diffusion is determined by the HT temperature. Ni diffuses to the  $\beta$ -Ti grains of the Ti-6Al-4V alloy. Therefore, the presence of  $\beta$ -Ti in the Ti alloy substrates becomes more pronounced, while the films are mainly formed by the NiTi<sub>2</sub> intermetallic phase, although after deposition they had a near equiatomic overall chemical composition. Regarding Ni diffusion, no significant differences were detected for the two multilayer periods studied. The W interlayer deposited between bulk Ti-6Al-4V and multilayer thin film was too thin to prevent Ni diffusion. Nevertheless, the results indicate that W can be used as a diffusion barrier, which should be taken into consideration when using Ni/Ti multilayer thin films as fillers for joining Ti alloys, such as Ti-6Al-4V. This point must be confirmed with further scientific evidence.

**Author Contributions:** A.J.C., A.S.R., and M.T.V. conceived the experiments; A.J.C. produced the Ni/Ti multilayers and performed the EPMA analyses together with M.T.V.; A.J.C., A.S.R. and F.B.F. carried out the synchrotron experiments, with the support of the beamline scientist C.B.; A.J.C. and A.S.R. wrote the manuscript (with contributions from all the other co-authors).

**Funding:** This research was sponsored by FEDER funds through the program COMPETE 2020 and National Funds through FCT-Portuguese Foundation for Science and Technology, which provided financial support for CEMMPRE under the project UID/EMS/00285/2013, and for CENIMAT/I3N under project number UID/CTM/50025 and SciTech Science and Technology for Competitive and Sustainable Industries. The R&D project was co-financed by Programa Operacional Regional do Norte (“NORTE2020”). The authors would like to thank FCT for the grant SFRH/BPD/109788/2015. The authors also acknowledge ESRF funding of the experiment at the ESRF MA-1985 entitled “In-situ phase evolution of sputtered reactive multilayers: Effect of the substrate”.

**Conflicts of Interest:** The authors declare no conflict of interest.

#### References

1. Boyer, R.R. An overview on the use of titanium in the aerospace industry. *Mater. Sci. Eng.* **1996**, *A213*, 103–114. [[CrossRef](#)]
2. Leyens, C.; Peters, M. *Titanium and Titanium Alloys*; Wiley-VCH: Weinheim, Germany, 2003.
3. Zoeram, A.S.; Mousavi, S.A.A.A. Laser welding of Ti-6Al-4V to nitinol. *Mater. Des.* **2014**, *61*, 185–190. [[CrossRef](#)]
4. Miranda, R.M.; Assunção, E.; Silva, R.J.C.; Oliveira, J.P.; Quintino, L. Fiber laser Welding of NiTi to Ti-6Al-4V. *Int. J. Adv. Manuf. Technol.* **2015**, *81*, 1533–1538. [[CrossRef](#)]
5. Oliveira, J.P.; Panton, B.; Zeng, Z.; Andrei, C.M.; Zhou, N.; Miranda, R.M.; Fernandes, F.M.B. Laser Joining of NiTi to Ti6Al4V using a Niobium interlayer. *Acta Mater.* **2016**, *105*, 9–15. [[CrossRef](#)]
6. Shiue, R.K.; Wu, S.K.; Chen, Y.T.; Shiue, C.Y. Infrared brazing of Ti50Al50 and Ti-6Al-4V using two Ti-based filler metals. *Intermetallics* **2008**, *16*, 1083–1089. [[CrossRef](#)]

7. Cao, J.; Song, X.G.; Li, C.; Zhao, L.Y.; Feng, J.C. Brazing ZrO<sub>2</sub> ceramic to Ti–6Al–4V alloy using NiCrSiB amorphous filler foil: Interfacial microstructure and joint properties. *Mater. Charact.* **2013**, *81*, 85–91. [[CrossRef](#)]
8. Ferrante, M.; Pigoretti, E.V. Diffusion bonding of Ti6Al4V to AISI 316L stainless steel: Mechanical resistance and interface microstructure. *J. Mater. Sci.* **2002**, *37*, 2825–2833. [[CrossRef](#)]
9. Kundu, S.; Sam, S.; Chatterjee, S. Interface microstructure and strength properties of Ti6Al4V and microduplex stainless steel diffusion bonded joints. *Mater. Des.* **2011**, *32*, 2997–3003. [[CrossRef](#)]
10. Kundu, S.; Sam, S.; Mishra, B.; Chatterjee, S. Diffusion bonding of microduplex stainless steel and Ti alloy with and without interlayer: Interface microstructure and strength properties. *Metall. Mater. Trans.* **2014**, *45A*, 371–383. [[CrossRef](#)]
11. Balasubramanian, M. Characterization of diffusion-bonded titanium alloy and 304 stainless steel with Ag as an interlayer. *Int. J. Adv. Manuf. Technol.* **2016**, *82*, 153–162. [[CrossRef](#)]
12. Simões, S.; Viana, F.; Ramos, A.S.; Vieira, M.T.; Vieira, M.F. Reaction zone formed during diffusion bonding of TiNi to Ti6Al4V using Ni/Ti nanolayers. *J. Mater. Sci.* **2013**, *48*, 7718–7727. [[CrossRef](#)]
13. Cavaleiro, A.J.; Ramos, A.S.; Fernandes, F.M.B.; Schell, N.; Vieira, M.T. In Situ Characterization of NiTi/Ti6Al4V Joints During Reaction-Assisted Diffusion Bonding Using Ni/Ti Multilayers. *J. Mater. Eng. Perform.* **2014**, *23*, 1625–1629. [[CrossRef](#)]
14. Cavaleiro, A.J.; Ramos, A.S.; Vieira, M.T.; Martins, R.M.S.; Fernandes, F.M.B.; Morgiel, J.; Baetz, C. Phase transformations in Ni/Ti multilayers investigated by synchrotron radiation-based x-ray diffraction. *J. Alloys Compd.* **2015**, *646*, 1165–1171. [[CrossRef](#)]
15. Cavaleiro, A.J.; Santos, R.J.; Ramos, A.S.; Vieira, M.T. In-situ thermal evolution of Ni/Ti multilayer thin films. *Intermetallics* **2014**, *51*, 11–17. [[CrossRef](#)]
16. Chen, Y.; Liu, S.; Zhao, Y.; Liu, Q.; Zhu, L.; Song, X.; Zhang, Y.; Hao, J. Diffusion behavior and mechanical properties of Cu-Ni coating on TC4 alloy. *Vacuum* **2017**, *143*, 150–157. [[CrossRef](#)]
17. Bitzer, M.; Bram, M.; Buchkremer, H.P.; Stöver, D. Phase transformation behavior of hot isostatically pressed NiTi-X (X = Ag, Nb, W) alloys for functional engineering applications. *J. Mater. Eng. Perform.* **2012**, *21*, 2535–2545. [[CrossRef](#)]
18. Gupta, R.; Gupta, M.; Kulkarni, S.K.; Kharrazi, S.; Gupta, A.; Chaudhari, S.M. Thermal stability of nanometer range Ti/Ni multilayers. *Thin Solid Films* **2006**, *515*, 2213–2219. [[CrossRef](#)]
19. Hubbel, J.H.; Seltzer, S.M. *Tables of X-ray Mass Attenuation Coefficients and Mass Energy-Absorption Coefficients from 1 keV to 20 MeV for Elements Z = 1 to 92 and 48 Additional Substances of Dosimetric Interest*; NIST Interagency/Internal Report (NISTIR): Gaithersburg, MD, USA, 1995.



© 2018 by the authors. Licensee MDPI, Basel, Switzerland. This article is an open access article distributed under the terms and conditions of the Creative Commons Attribution (CC BY) license (<http://creativecommons.org/licenses/by/4.0/>).